This document is the accepted manuscript version of the following article:
Vandenbossche, M., Petit, L., Mathon-Lagresle, J., Spano, F., Rupper, P., Bernard, L., & Hegemann, D. (2018). Formation of lateral chemical gradients in plasma polymer films shielded by an inclined mask. Plasma Processes and Polymers, e1700185 (10 pp.). http://doi.org/10.1002/ppap.201700185

Formation of lateral chemical gradients in plasma polymer films shielded by an inclined mask

M. Vandenbossche[1*], L. Petit[1], J. Mathon-Lagresle[1], F. Spano[2], P. Rupper[1], L. Bernard[3], D. Hegemann[1]

[1]*Laboratory of Advanced Fibers, Empa, Swiss Federal Laboratories for Materials Science and Technology, Lerchenfeldstrasse 5, 9014 St. Gallen, Switzerland*
[2]*Laboratory for Biomimetic Membranes and Textiles, Empa, Swiss Federal Laboratories for Materials Science and Technology, Lerchenfeldstrasse 5, 9014 St. Gallen, Switzerland*
[3]*Laboratory for Nanoscale Materials Science, Empa, Swiss Federal Laboratories for Materials Science and Technology, Überlandstrasse 129, 8600 Dübendorf, Switzerland*

*Corresponding author: Marianne Vandenbossche, vdb.m22@gmail.com

Abstract

Low pressure plasma deposition conditions were investigated yielding oxygen-containing lateral gradient coatings (a-C:H:O) by means of an inclined static mask partly shielding the substrate. The transition from direct plasma exposure to remote plasma polymer film (PPF) growth can thus be studied which is, e.g., important for reel-to-reel processes (sample leaving the plasma zone) and coating of soft materials (avoiding harsh plasma conditions). Such lateral gradient coatings were formed by the diffusion of film-forming species with different reactivities underneath the mask. Surface characterization of the lateral gradient revealed varying film growth conditions below the mask with increasing distance from the mask/plasma edge: i) exponentially decreasing film growth; ii) decreasing roughness following the thickness trend; iii) decreasing hydrophilicity; iv) variation in cross-linking; and v) different chemical composition. The latter can be divided into three main areas: 1) the unmasked area (plasma exposed), with $[O]_{PPF}/[C]_{PPF} \sim 19\%$; 2) the first 1 cm below the mask close to the mask/plasma edge with $[O]_{PPF}/[C]_{PPF} \sim 26\%$; and 3) the fully masked area, with $[O]_{PPF}/[C]_{PPF} \sim 13\%$. Thus, oxygen-rich film-forming species appeared to react closer to the mask/plasma edge, while oxygen-poor film-forming species can diffuse deeper, leading to a pronounced gradient in chemical composition and in cross-linking in the masked area.

Key-words

Plasma polymerization, lateral gradient structure, static mask, film-forming species, diffusion.

Introduction

Preparation of lateral chemical gradients gained great interest since middle of the 20th century. [1] Indeed, surfaces that contain a gradient in chemical composition or structure are known to provide an excellent platform to study many concurrent surface properties in an efficient manner.[2] Thus, lateral gradients were extensively used for numerous practical applications, such as the investigation of biomolecular interactions, cell-mobility studies, diagnostics, nano-tribology, and microfluidics.[3] Two main strategies were developed in order to produce lateral chemical gradients: top-down and bottom-up methods. Top-down methods consist in progressively modifying chemically or physically the surface of the substrate,[4] whereas the bottom-up methods are based on depositing gradually some monomers, oligomers or polymers.[5] As bottom-up methods depend less on the nature of the substrate, such a method was selected in this study.

Two main process configurations are normally used to produce a lateral gradient. The first one is the static configuration, in which the substrate (and mask, if used) is fixed. This way, the lateral gradient is produced due to diffusion of active species along the shielded surface of the substrate. The second one is the dynamic configuration, in which the substrate and/or the mask is moving and varying the plasma exposure time to produce gradients along the surface of the substrate.[6] As the dynamic configuration corresponds to a succession of various static configurations, an in-depth investigation on the formation of lateral gradients produced by the static configuration becomes relevant not only to understand the diffusion phenomenon in such configuration, but also to (partly) explain the mechanism occurring in dynamic situations such as in reel-to-reel processes.

Lateral chemical gradients can be prepared by wet chemistry as well as chemical vapor deposition. However, there are some restrictions for most methods to prepare soft matter gradients as reported by Zelzer et al.,[7] "*plasma polymerization is so far the only method for*

the preparation of soft matter gradients that is not restricted to a specific substrate or functional group". Thanks to the high stability of plasma polymer films (PPFs),[8,9,10] and to the ability to coat complex 3D objects with PPFs, the plasma technique becomes more and more prominent for biomedical applications.[5,7,11] However, the final PPF structure might be affected by the process used to provide the lateral gradient at the surface of a substrate, leading to different film properties than initially expected. Indeed, plasma deposition is governed by gas phase and surface reaction processes. In the gas phase, precursors (or monomers) dissociate and can then recombine, generating the so-called film-forming species. Neutral film-forming species diffuse in the plasma chamber to deposit onto the substrate surfaces (and all other available surfaces). Note that these film-forming species might react again while diffusing in the plasma chamber, due to the high density of energetic particles in the plasma zone, also including charge-transfer reactions. At the substrate surface, ions bombard the forming PPF, after being accelerated through the plasma sheath mainly following the direction of the electric field. Ion bombardment supports formation of radical sites and surface cross-linking but also surface etching. Thus, using a mask to partly shield a sample from direct plasma exposure, which is sufficiently separated from the substrate to allow diffusion of film-forming species, the formation of a lateral gradient is expected: ions will bombard only the uncovered area leading to different chemical compositions and different cross-linking degrees along the substrate surface.

When a substrate is covered with a one-end open mask, a constant diffusion rate of the plasma reactive species is obtained.[12] Mangindaan *et al*. started to determine the mechanism related to the production of lateral gradients onto polypropylene substrates using such a mask in the static configuration.[13] A model consisting of three sub-processes was proposed: 1) bulk diffusion of the plasma reactive species, 2) interfacial adsorption/desorption and 3) surface chemical reactions. Thanks to their model, for which the third step was specific to SF_6 plasmas onto polypropylene substrates, the authors explained the gradual wetting properties

along the substrate surface. However, the substrate on which the plasma-based lateral gradient is deposited might be a metal or metal-oxide material, as well (for example, a gold-coated sensor for bio-sensing purpose). In this case, mainly one chemical reaction at the surface is expected: the formation of Metal-O-C bonds when the film-forming species adhere onto the substrate surface.[14] This is the reason why it becomes interesting to examine whether gradual wetting properties can also be observed while preparing a plasma-based lateral gradient in the static configuration, and if so, to understand the mechanism to better control the deposition of such gradient films.

In this study, Si wafer substrates were partially protected by an inclined mask in order to avoid ion bombardment (from the applied low pressure plasma) below the shielded area. Thus, plasma deposition of the a-C:H:O films below the mask is expected to be mainly driven by diffusion of neutral film-forming species. Wetting properties, thickness and topography were determined along the lateral gradient. Finally, the lateral chemical gradient was identified by X-ray photoelectron spectroscopy (XPS) and time-of-flight secondary ion mass spectrometry (ToF-SIMS) indicating three distinct areas along the oxygen-containing PPF.

Materials and methods

Plasma deposition of the lateral gradient coating

A cylindrical and symmetric plasma reactor with two plane parallel electrodes (30 cm in diameter) separated by a glass ring (5 cm in height) was used to deposit plasma polymer films (PPFs) at low pressure. The upper electrode contained a gas showerhead, while the chamber was pumped through the lower electrode which was capacitively coupled to the RF generator (13.56 MHz) enabling well-defined deposition conditions.[15] Previously optimized conditions were selected to deposit functional yet stable PPFs.[15,16] For the deposition of the carboxylic acid-containing PPF onto Si wafer substrates (5 cm x 1.5 cm, 1 mm height), the

discharge was carried out in a mixture of CO_2/C_2H_4, with flow rates of 8 and 4 sccm, respectively (gas flow ratio 2:1), a pressure of 10 Pa, and a power input of 50 W. In order to generate a lateral gradient in the deposited a-C:H:O film, a rigid PET sheet (7 cm x 5 cm) tilted at an angle of ~4° was placed over the silicon wafer to provide an inclined mask (Figure 1). In this way, the mask had a maximum distance of 5 mm from the electrode, while the other end touched the electrode (closed-end). Note that Si wafers were cleaned by Ar plasma (10 min, 50 W, 10 Pa) prior to placing the mask and plasma deposition.

After plasma treatment, samples were immediately stored in the dark in sterile Petri dish boxes at 24°C and 60% of humidity. Analyses were carried out within the first hour after plasma deposition.

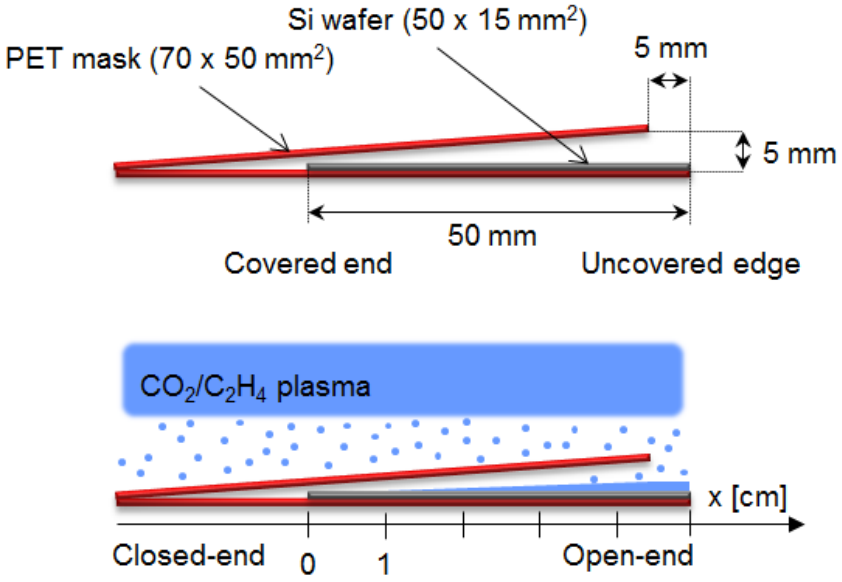

Figure 1. Scheme of the experimental setup used to prepare a lateral gradient by diffusion of film-forming species in a CO_2/C_2H_4 plasma. The sample was placed onto the bottom (driven) electrode in the plasma chamber.

Kinetic study on the growth of the lateral gradient coating

The setup presented in Figure 1 was used to prepare different lateral gradient coatings by varying deposition duration: 10 min, 20 min, 30 min, 45 min, and 60 min. For each sample (at least 2 samples for each type of coating and per analysis method) the thickness of the

coating along the gradient and wetting properties were determined. Surface chemical analyses XPS and ToF-SIMS were carried out on the sample treated for 30 min.

Thickness measurements along the lateral gradient coating

A thin adhesive strip (2-3 mm width) was put along the length of the silicon wafer sample during plasma deposition to protect this part from coating (this protected part constitutes the zero-level (z = 0) for further thickness measurements). After removing the adhesive, the thickness of the coating at different positions, *i.e.* at x = 1, 2, 2.5, 3, 3.5, 3.8, 4.0, 4.3, 4.5, 4.8, and 5 cm from the closed-end of the mask (where x = 4.5 cm corresponds to the mask/plasma edge), was measured using a profilometer (Veeco Dektak 150). Line profiles crossing the film edge (500 µm long) were thus carried out using a silicon oxide stylus (diameter of 2.5 µm) with an applied force of 3.0 mg for 15 s.

Water contact angle measurements along the lateral gradient coating

Static water contact angle (WCA) was measured in ambient atmospheric conditions onto freshly prepared samples using the static sessile drop method. To determine the WCA, at least two drops (2 µL) of water (CHROMASOLV®, for HPLC, Sigma Aldrich) were put at different positions on the surface of the lateral gradient and analyzed using the software controlled drop shape analyser (DSA25, Krüss). In addition, WCA measurements were repeated after 4 months aging in air.

Determination of topography along the lateral gradient coating

Information on the topography (roughness) at different positions of the lateral gradient structure was obtained by atomic force microscopy (AFM). The AFM analysis was conducted by means of a scanning probe microscope FlexAFM V5 (from Nanosurf AG, Liestal, Switzerland) equipped with a C3000 controller and the associated software. The measurements were performed in tapping mode. Areas of 1 x 1 μm^2 were scanned using a pyramidal silicon tip with a resonance frequency of 190 kHz and a spring constant of 48 N/m (BudgetSensors,

Tap190Al-G). AFM images were analyzed using the open-source software Gwyddion 2.45.[17] First, a two-dimensional levelling of the data was carried out by mean plane subtraction, followed by aligning the rows using a first order polynomial method. Finally, the minimum data value was shifted to zero. After image treatment, the RMS roughness average (Sq) was calculated by Gwyddion. Results obtained at different positions along the lateral gradient were compared to the topography of a pristine Si wafer previously washed and sonicated in ethanol for 15 min, and cleaned in Ar plasma for 10 min.

XPS analysis along the lateral gradient coating

The chemical composition of the lateral gradient structure prepared for 30 min in the plasma chamber was analyzed at different positions (x = 1, 2, 2.5, 3, 3.5, 3.8, 4.0, 4.3, 4.5, 4.8, and 5 cm from the closed-end of the mask) by XPS measurements using a Scanning XPS Microprobe (PHI VersaProbe II spectrometer, Physical Electronics) with monochromatic Al Kα radiation (1486.6 eV). The operating pressure of the XPS analysis chamber was below 5 x 10^{-7} Pa during the measurements. The spectra were collected at photoemission take-off angles of 45^{o} (with respect to the sample surface). Survey scan spectra (0 – 1100 eV) were acquired with an energy step width of 0.8 eV, acquisition time of 160 ms per data point and analyzer pass energies of 187.85 eV. Higher resolution narrow spectra over carbon C1s, oxygen O1s and silicon Si2p regions were acquired with a pass energy of 29.35 eV and an energy step width of 0.125 eV.

Measurements were carried out using a micro-focused X-ray beam with a diameter of 100 μm (25 W at 15 kV). The 180^{o} spherical capacitor energy analyzer was operated in the fixed analyzer transmission mode (FAT). In order to compensate possible sample charging, dual beam charge neutralization with a flux of low energetic electrons (~1 eV) combined with very low energy positive Ar ions (10 eV) was used. Obtained spectra were rescaled by shifting the spectra relative to the aliphatic carbon at

285.0 eV. Curve fitting (least-squares fit routines) with CasaXPS software version 2.3.16 was employed to calculate the atomic concentrations. A mixed Gaussian-Lorentzian product function (constant ratio of 70% Gaussian and 30% Lorentzian) was used to de-convolute the XP spectra and a Shirley type background was subtracted from the XPS peak areas. For quantification, PHI sensitivity factors[18] were corrected for our system's transmission function and spectrometer geometry (asymmetry function).

ToF-SIMS analysis along the lateral gradient coating

ToF-SIMS measurements (ToF-SIMS.5 instrument, IONTOF, Germany) were carried out in order to evaluate the cross-linking degree along the lateral gradient coating (prepared for 30 min). 50 keV Bi_3^{++} primary ions in the high mass resolution mode were used to analyze the PPF topmost surface (first few monolayers) on areas of 200×200 μm^2. All negatively charged secondary ions from 1 to 550 atomic mass units were detected (typical sensitivity in the ppm range). 11 positions between 0.2 cm and 4.8 cm along the sample were analyzed, and sets of 12 measurements per position were acquired to obtain a representative statistics.

Results

Ahead of the preparation of lateral gradients, an amorphous oxygen-containing PPF (a-C:H:O) was prepared by plasma polymerization with the pre-selected conditions (gas flow ratio CO_2/C_2H_4 8:4, 50 W, 10 Pa) onto Si wafer substrates to determine deposition rate and water contact angle (WCA) of such coatings in unmasked (usual plasma-exposed) deposition conditions. A deposition rate of 7.4 ± 0.2 nm/min and a WCA of 47 ± 2° were obtained.

An inclined mask was then placed in the plasma chamber at a maximum distance of 5 mm above the electrode (at the open-end, i.e. the mask/plasma edge). Note that the optical visible sheath thickness was about 10 mm, as previously observed in the same plasma conditions.[16] Therefore, the mask was entirely immersed in the sheath area.

Different lateral gradient structures were prepared by varying plasma deposition time from 10 to 60 min. WCA as well as thickness values of the coatings are reported in Figure 2. First of all, a gradient regarding surface wettability was observed for all the prepared samples (Figure 2a). WCA values of ~50° were measured for all gradient coatings in the open-end area close to the mask/plasma edge. As observed in Figure 2a, WCA values were found to be higher below the mask and increased for further 2-3 cm starting from the open-end towards the closed-end side (x = 0 of the Si wafer). Note that after 4 months aging in air, the same WCA values along the gradient were obtained, showing stable wetting properties of the coating when stored in air.

Regarding the thickness of the coating at different positions on the substrate, a regular pattern can be observed related to the deposition duration. In the unmasked area, from x = 4.5 to 5.0 cm, the deposition rate seems to be affected by the presence of the mask, as the measured thickness was lower than observed for direct plasma exposure without masking (Figure 2b). Indeed, a deposition rate of 6.8 ± 0.2 nm/min was measured at 5 mm distance from the mask/plasma edge (compared to 7.4 nm/min). This result is directly linked to the presence of

the mask that partially hinders the diffusion of the neutral film-forming species (Figure S1), and thus, some film-forming species are shielded by the mask. Moreover, some ions could bombard the edge of the mask and be reflected toward the unmasked surface of the Si wafer, leading to slightly more etching in the unmasked area compared to usual deposition conditions.

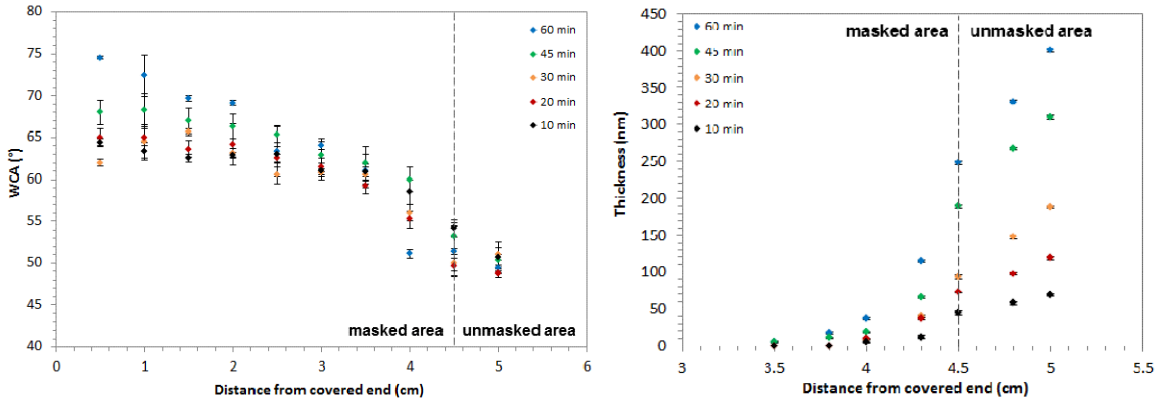

(a) (b)

Figure 2. Evolution of water contact angle (a) and coating thickness (b) along lateral gradient coating prepared according to different plasma deposition times: 10 min, 20 min, 30 min, 45 min, and 60 min. Note that x = 0 corresponds to the covered end.

As indicated by the strongly decreasing deposition rate underneath the mask, the diffusion of the neutral film-forming species was mainly confined to the area extending over approximately 1 cm below the mask (Figure 2b; note that for ultrathin coatings, i.e. <10-15 nm, the thickness was difficult to measure by profilometry).

Kinetic studies have been carried out to characterize the plasma polymer growth at different positions below the mask. Figure 3 plots the evolution of the coating thickness as a function of the plasma deposition time for each position from x = 3.8 to 5 cm. Since a linear trend was observed for all positions, steady film growth conditions were revealed, similarly to what is known for direct plasma exposure. The following constant deposition rates can thus be given for each position: 0.27 ± 0.04 nm/min at x = 3.8 cm, 0.6 ± 0.1 nm/min at 4.0 cm,

1.8 ± 0.2 nm/min at 4.3 cm, 4.1 ± 0.3 nm/min at 4.5 cm, 5.6 ± 0.3 nm/min at 4.8 cm, and 6.8 ± 0.2 nm/min within the unmasked area at 5 cm (Table 1 and Figure 4).

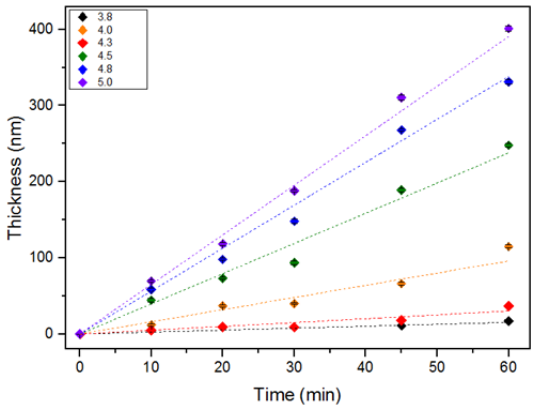

Figure 3. Evolution of the coating thickness as a function of the plasma deposition duration at different distances from the covered end of the mask (x = 0): 3.8, 4, 4.3, 4.5, 4.8, and 5 cm.

Table 1. Deposition rate values at different distances from the covered end (x = 0): 3.8, 4.0, 4.3, 4.5, 4.8, and 5.0 cm (extracted from Figure 3), as well as the standard error associated to each deposition rate value and the correlation coefficient.

Linear fit	**Distance from covered end (x = 0) (cm)**					
	3.8	4.0	4.3	4.5	4.8	5.0
Slope (nm/min)	0.27	0.6	1.8	4.1	5.6	6.8
Standard error (nm/min)	0.04	0.1	0.2	0.3	0.3	0.2
R^2	0.97	0.86	0.94	0.97	0.98	0.995

Below the mask, the deposition rate (R), considered for different positions, followed an exponential function ($R^2 = 0.9995$), that can be written as $R_m = R_0\, e^{kx}$ with a fitted deposition rate $R_0 = 9.7\ 10^{-8}$ nm/min (deposition rate for x = 0), and k = 3.9 cm^{-1} (with k the growth rate gradient along the sample underneath the masked area). According to this model (Figure S2, supplementary information), a film growth can be expected all over the sample surface. However, heterogeneous, i.e. non-continuous coating formation can be assumed during initial growth dominating at the covered end of the mask.[9]

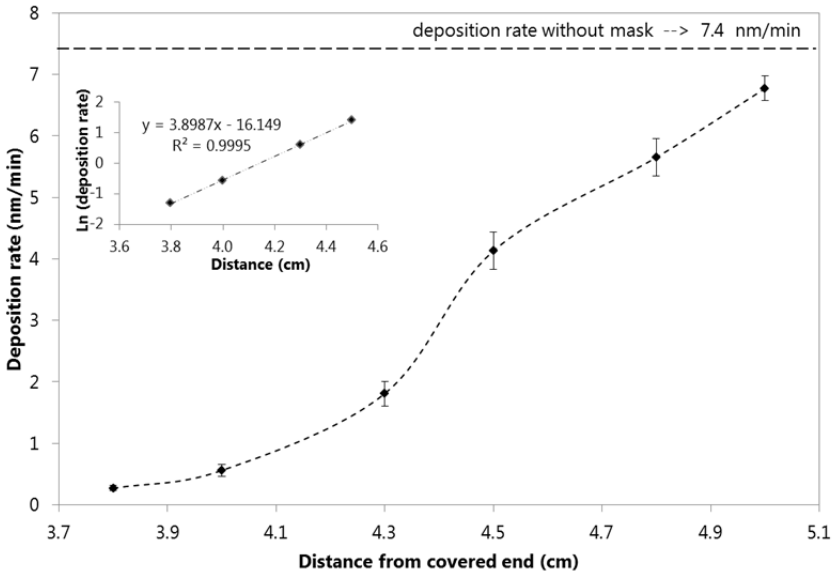

Figure 4. Plasma polymer film deposition rate at different distances from the covered end (x = 0): 3.8, 4.0, 4.3, 4.5, 4.8, and 5.0 cm. Deposition rate below the mask fits very well with an exponential function, as observed on the inset sketch.

To confirm the presence of a plasma polymer film at short distances from the covered end of the mask, AFM was used to measure the topography of coated and pristine Si wafer surfaces (Figure 5). A clear structural change was obtained for different coated positions underneath the mask. First of all, evidence of the presence of a plasma polymer film was given by a higher roughness measured for the coated samples compared to the pristine Si wafer (0.12 ± 0.03 nm). For positions underneath the mask ranging from x = 0 to 3.5 cm, a constant average roughness of S_q = 0.19 ± 0.03 nm was observed. Closer to the mask/plasma edge (according to increasing deposition rates) the roughness values increased to S_q = 0.25 ± 0.03 nm at x = 3.8 cm, S_q = 0.27 ± 0.03 nm at 4 cm, S_q = 0.33 ± 0.04 nm at 4.3 cm, until reaching the unmasked area (range from x = 4.5 cm to 5 cm) where the average roughness is about 0.39 ± 0.05 nm. Higher roughness in the unmasked area can be related to the direct plasma exposure yielding ion-induced etching effects during the deposition process.

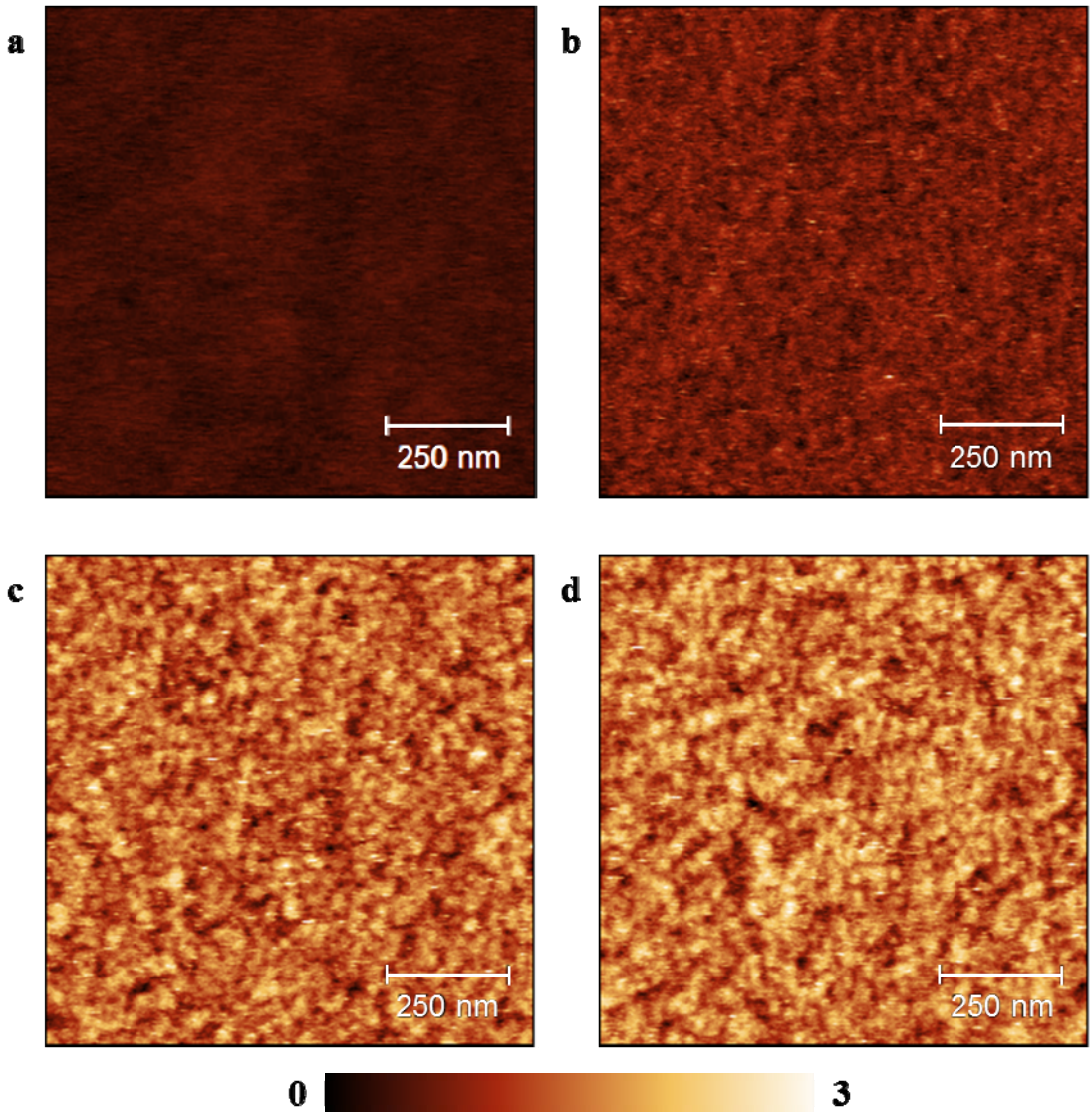

Figure 5. Topography of (a) the pure Si wafer (washed in ethanol and sonicated for 15 min, and then plasma cleaned for 10 min) and of the lateral gradient structure (prepared for 30 min plasma deposition time) at different positions: (b) x = 2 cm, (c) x = 4.5 cm and (d) x = 5 cm. Color scales are given in nanometer.

XPS analyses were carried out at different positions at the surface of the lateral gradient. Two main points should be highlighted from the obtained surveys (Figure 6 and Table 2): 1) the amount of oxygen was higher in the masked area than in the unmasked area; and 2) the amount of silicon (from the substrate) is negligible from x = 3.8 to 5.0 cm, but prominent for positions closer to the closed-end of the mask. Since our used Si wafer consists of SiO_2 at the surface, oxygen contribution from the sample should be considered for low plasma polymer film coverages.

A simple calculation was thus carried out by subtracting the amount of oxygen of the substrate from the total amount of oxygen, considering that $[O]_{Total} = [O]_{PPF} + [O]_{SiO2}$, with $[O]_{SiO2} = 2 \times [Si]$. By this way, a corrected [O]/[C] value was calculated indicating the oxygen/carbon ratio for the PPF (assuming that carbon was only originating from the PPF): $\frac{[O]_{PPF}}{[C]_{PPF}} = \frac{[O]_{Total} - 2*[Si]}{[C]_{Total}}$. Note that this correction implies an approximation regarding the purity of the substrate surface: we made the hypothesis that there was no contaminant at the surface of the substrate (samples were washed and plasma cleaned before film deposition) and that the oxygen was coming only from the homogeneous SiO_2 substrate surface or the PPF layer.

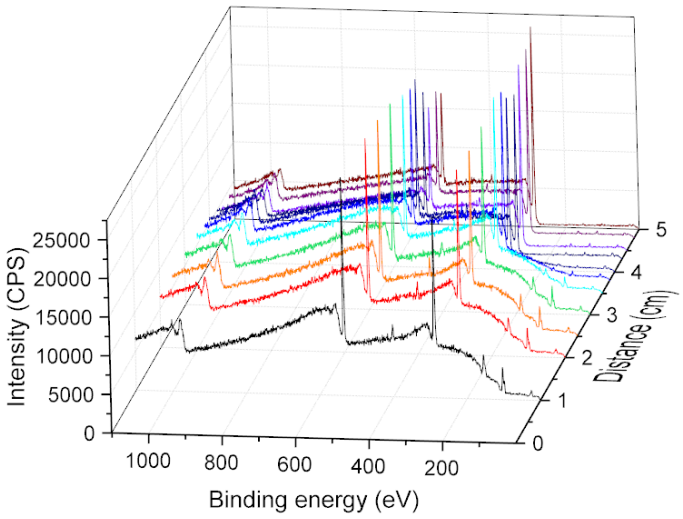

Figure 6. XPS survey spectra at different positions of the lateral gradient coating (x = 1.0, 2.0, 2.5, 3.0, 3.5, 3.8, 4.0, 4.3, 4.5, 4.8, and 5.0 cm).

Table 2. Atomic percentage of carbon, oxygen and silicon, as well as the [O]/[C] ratio and the corrected [O]/[C] ratio (named $[O]_{PPF}/[C]_{PPF}$), all given in [%], for the analyzed positions.

cm	C1s	O1s	Si2p	[O]/[C]	$[O]_{PPF}/[C]_{PPF}$
1.0	59.4	29.1	11.5	49.0	10.3
2.0	63.0	27.6	9.4	43.7	13.9

2.5	62.5	27.7	9.8	44.4	13.1
3.0	64.8	26.7	8.5	41.2	15.0
3.5	71.2	24.3	4.6	34.1	21.2
3.8	77.9	22.1	-	28.4	28.4
4.0	78.5	21.5	-	27.3	27.3
4.3	80.5	19.5	-	24.3	24.3
4.5	83.0	17.0	-	20.5	20.5
4.8	83.8	16.2	-	19.3	19.3

The $[O]_{PPF}/[C]_{PPF}$ ratios along the sample (Table 2 and Figure 7) have been used to highlight different areas. The unmasked area showed a chemical composition comparable to the coating as deposited without a mask (at x = 4.8 cm, [O]/[C] = 19.3%, compared to [O]/[C] ~ 22% [8]). The masked area can be divided into two parts: one region ranging from x = 3.5 to 4.5 cm and a second region ranging from x = 0 to 3.5 cm. As shown in Figure 7, enhanced $[O]_{PPF}/[C]_{PPF}$ ratios were measured in between x = 3.5 and 4.5 cm, whereas lower ratios were obtained from x = 0 to 3.5 cm. Moreover, after deconvolution of the C1s peak, the three areas related to different oxygen-containing chemical groups can be indicated (Figure 7) showing similar tendencies as for the corrected [O]/[C] ratios. Thus, a separation of the film-forming species according to their chemical compositions/reactivities was observed when these species diffused along the sample surface underneath the inclined mask.

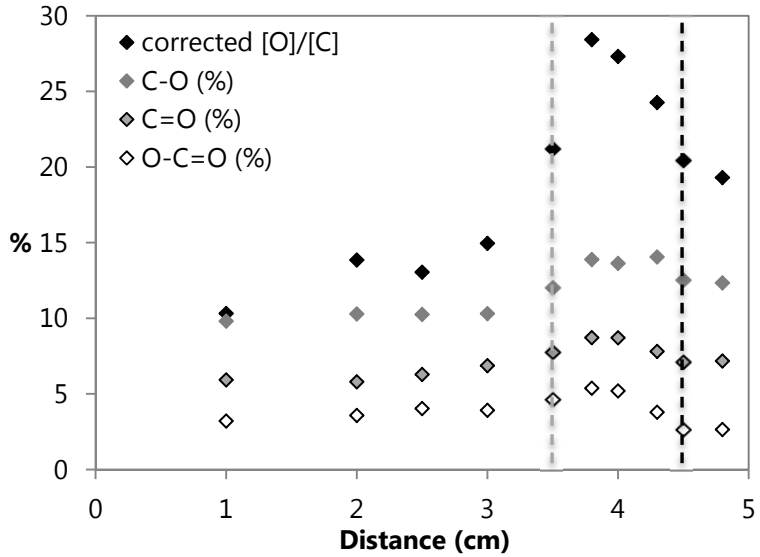

Figure 7. $[O]_{PPF}/[C]_{PPF}$ ratio (also named corrected [O]/[C]) at different positions of the lateral gradient showing three main areas, and concentration percentage of the C-O bonds, C=O bonds and O=C-O bonds, obtained by deconvolution of the C1s peak.

Further analyses were performed by ToF-SIMS. Figure 8 displays the [C]/[H] and the [O]/[C] ratios obtained along the lateral gradient coating deposited for 30 min. For each position, all fragments were summed, weighted by the C, H and O content and the peak intensity. Knowing that a higher [C]/[H] ratio is related to a higher cross-linking degree, we can deduce that the plasma polymer film is significantly more cross-linked in the unmasked area (slightly ranging below the mask to the position at x = 4.3 cm) than in the masked area. This result is explained by the presence (in the unmasked area) or the absence (in the masked area) of ions that bombard the surface. Note that the [C]/[H] ratio slightly increased for positions close to x = 0 cm, We attribute this to an apparent lower H content due to surface attachment of the polymer fragment onto the substrate, made visible to ToF-SIMS when the film thickness is in the range of few nanometers.

Regarding the oxygen content along the lateral gradient, a higher amount of oxygen can be noticed for positions located below the mask, compared to the positions located in the unmasked area, as it was previously observed by XPS. As less ion bombardment leads to more functionality, this result is in accordance with the result obtained for the [C]/[H] ratio. The higher amount of oxygen at some centimeters from the edge of the mask could thus be explained by the diffusion of oxygen-containing species below the mask. In addition, [O]/[C] ratio was slightly lower for positions close to x = 0, showing a separation of the species along the sample surface below the mask.

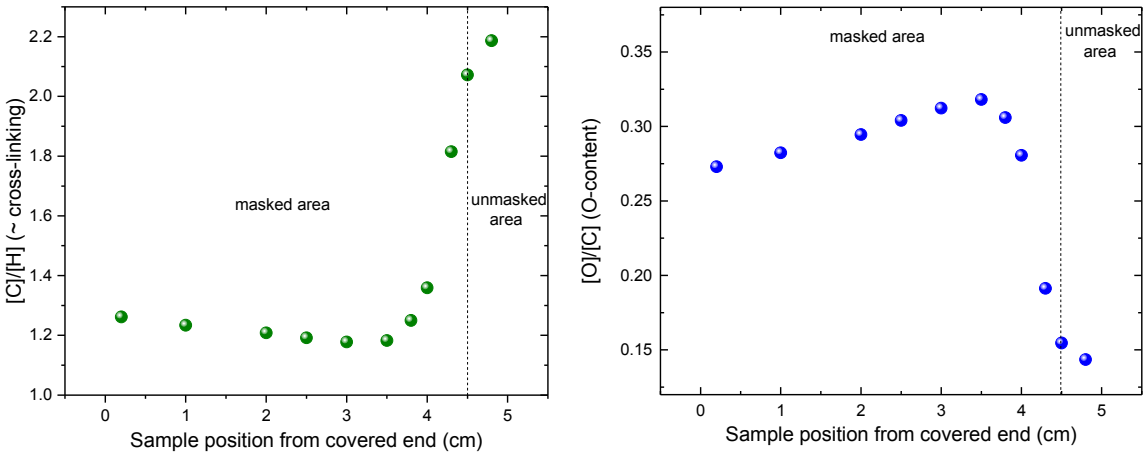

Figure 8. [C]/[H] and [O]/[C] ratios calculated at different positions along the lateral gradient coating by summing C, H and O for all fragments determined by ToF-SIMS, weighted by their peak intensity.

Discussion

As the sample is shielded from ion bombardment by the inclined mask (except for a few mm close to the mask/plasma edge), diffusion processes along the sample and plasma-chemical effects become dominant. Regarding the CO_2/C_2H_4 plasma used in this study, the identification of the film-forming species that may diffuse below the mask becomes necessary. Neutral film-forming species are created due to collisions with electrons in the (low pressure) plasma zone, leading to fragmentation of the monomer and of the reactive gas in the reactor. Electrons are known to be mostly responsible for the vibrational energy in the ground levels of CO_2 (the vibrational excited CO_2 molecule is hereafter written as CO_2*). When there is an excess of vibrational energy, the molecule dissociates according to the following reactions:[19] $CO_2^* \rightarrow CO + O$ (main reaction); and $O + CO_2^* \rightarrow CO + O_2$ (secondary reaction). Other chemical reactions may also occur in the plasma zone but with a lower probability. For example, the dissociative attachment of electrons would also contribute to the CO_2 decomposition in the plasma, according to the following reaction: $e^- + CO_2 \rightarrow CO + O^-$.

Atomic oxygen formed during CO_2 decomposition in the plasma is highly reactive. Thus, chain branching reaction of oxygen with ethylene is favored:[16,20] $O + C_2H_4 \rightarrow CH_3 + HCO$ and $O + C_2H_4 \rightarrow H + CH_2CHO$. In addition, it was previously

shown that for low deposition rate, atomic oxygen was responsible for most of the reactions at the coating surface that increases the surface energy as well as for chemical etching.[21] Other reactions might occur in the plasma zone, following the formation of acetylene by electron impact onto ethylene[20] and sequential reactions between hydrocarbon radicals and stable molecules present in the gas phase.[22] Thus, hydrocarbons and oxygen-containing fragments, and above all atomic oxygen, are the potential film forming species that would be able to diffuse below the mask during plasma deposition.

A lateral gradient in chemical composition was observed along the masked area (Figures 7 and 8) showing an enhanced $[O]_{PPF}/[C]_{PPF}$ ratio in the region from x = 3.8 to 4.3 cm close to the open-end of the mask, even higher than in the unmasked area (Table 2). As oxygen-containing fragments are known to be more reactive, they predominantly contribute to film growth in this region. For direct plasma exposure, a competitive deposition/ablation process can be assumed, where ion-induced etching and cross-linking explain the lower amount of oxygen observed in the unmasked area. For the masked area with less energetic conditions during film growth, the nucleation density on the sample surface becomes an important factor determining the deposition of film-forming species depending on their reactivity. The higher $[O]_{PPF}/[C]_{PPF}$ ratio from x = 3.8 to 4.3 cm from the covered end of the mask might thus be explained by a preferential adsorption of oxygen-rich film-forming species, whereas carbon-rich film-forming species (with lower reactivities) diffuse further along the sample surface. Therefore, the hydrocarbon content increased towards the closed-end of the mask and the deposition rate decreased exponentially. Accordingly, the WCA was found to be higher in this region giving rather constant values (of around 65°) in between x = 0 and 3 cm. The extremely thin hydrocarbon-rich layers in this region (with constant low roughness) showed low cross-linking, which slightly increased for decreasing thickness (close to the covered end of the mask) which might be substrate-related effect (Figure 8).

A different behavior was observed for the oxygen-rich PPFs deposited close to the open-end in between x = 3.5 and 4.5 cm. Despite a higher [O]/[C] ratio, the WCA were less hydrophilic compared to the ones measured in the unmasked area (Figure 2). Furthermore, ToF-SIMS indicates decreasing cross-linking with the distance from the mask/plasma edge below the mask, in agreement with the trend in roughness as observed by AFM.

In the absence of ion bombardment, chemical etching effects should be considered. Most of all, reactive species such as atomic oxygen are present in the region below the mask close to the open-end that induce chemical reactions at the coating surface. Such chemical etching processes support the release of small hydrocarbon fragments leading to an increase of the [O]/[C] ratio. The new chemical groups formed due to the oxygen chemical etching are thus expected to be rather non-polar, as the water contact angle was found to be higher (Figure 2).

Shielded plasma deposition conditions result in the growth of less (polar) functional and less cross-linked PPFs exhibiting a lateral gradient (in thickness, wettability, chemistry, roughness, cross-linking) with the distance from the direct plasma exposure. Nevertheless, such PPFs with increased [O]/[C] content indicating ester and ether group formation could be interesting as degradable surface layers deposited on sensitive substrates such as scaffolds etc.[23]

The results might also be important for remote plasma conditions, e.g. in reel-to-reel processes when a sample is transported through the plasma zone.[24] By leaving the plasma area, the coating might be terminated by a layer corresponding to the conditions using a mask. Considering, however, the low deposition rate in this zone (here around 1 nm/min), only slow processes (below 0.1 m/min) will be affected.

Conclusion

A lateral chemical gradient was formed by partly covering the substrate with an inclined mask. Evidence of gradients in wettability, thickness and roughness was given by an extensive surface characterization study. An evolution regarding the chemical composition was also observed by XPS and ToF-SIMS: the composition in oxygen along the gradient was found not to follow a linear function, and was higher at positions in between x = 3.5 and 4.5 cm close to the mask/plasma edge, which is related to a lower cross-linking degree.

Even if the mechanism is not yet fully understood, important aspects can be highlighted. Ion bombardment plays an important role during plasma deposition in the unmasked area, leading to a more cross-linked yet still functional plasma polymer film (PPF). Diffusion of the film-forming species occurred below the mask leading to the formation of less cross-linked PPFs with increased water contact angle values. In addition, two distinguished areas were observed: from x = 0 to 2 cm, a slightly more cross-linked and hydrocarbon rich (corrected [O]/[C] ~ 13%); and from x = 2 to 4.5 cm, a slightly less cross-linked and oxygen-rich (corrected [O]/[C] ≥ 20%) PPF.

To explain the presence of these two areas, diffusion of film-forming species was considered. First of all, film-forming species diffuse in the gas phase, more precisely in the volume above the sample (bulk diffusion). These film-forming species start to physically adsorb onto the surface depending on their reactivity. The nucleation density at the surface of the sample can then explain the results obtained by XPS and ToF-SIMS. Indeed, more reactive oxygen-rich film forming species can bind more readily onto the Si wafer substrate than oxygen-poor film-forming species. Thus, oxygen-poor film-forming species were found to diffuse further along the surface before they form a PPF with extremely low deposition rate. This would explain the XPS results along the lateral gradient, as well as the results obtained by ToF-SIMS. Furthermore, it can be inferred that samples that are transported through a plasma tend to collect a less cross-linked, oxygen-rich surface termination layer by leaving the zone

of the direct plasma exposure, which might, however, only be considered for rather low process velocities (<0.1 m/min).

Acknowledgements

The authors gratefully acknowledge the Swiss National Science foundation (SNSF, Bern) for funding this study under grant no. IZ73Z0_152661 (SCOPES).

References

[1] J. Genzer, R.R. Bhat, *Langmuir* **2008**, 24, 2294.

[2] D.J. Menzies, M. Jasieniak, H.J. Griesser, J.S. Forsythe, G. Johnson, G.A. McFarland, B.W. Muir, *Surf. Sci.* **2012**, 606, 1798.

[3] [3a] N. Ballav, A. Shaporenko, A. Terfort, M. Zharnikov, *Adv. Mater.* **2007**, 19, 998; [3b] S. Morgenthaler, S. Lee, S. Zürcher, N.D. Spencer, *Langmuir* **2003**, 19, 10459; [3c] K. Loos, S.B. Kennedy, N. Eidelman, Y. Tai, M. Zharnikov, E.J. Amis, A. Ulman, R.A. Gross, *Langmuir* **2005**, 21, 5237.

[4] H.T. Spijker, R. Bos, W. van Oeveren, J. de Vries, H.J. Busscher, *Colloid Surface B* **1999**, 15, 89.

[5] F.J. Harding, L.R. Clements, R.D. Short, H. Thissen, N.H. Voelcker, *Acta Biomater.* **2012**, 8, 1739.

[6] J.D. Whittle, D. Barton, M.R. Alexander, R.D. Short, *Chem. Commun.* **2003**, 9, 1766.

[7] M. Zelzer, D. Scurr, B. Abdullah, A.J. Urquhart, N. Gadegaard, J.W. Bradley, M.R. Alexander, *J. Phys. Chem. B* **2009**, 113, 8487.

[8] D. Hegemann, E. Lorusso, M.-I. Butron Garcia, N.E. Blanchard, P. Rupper, P. Favia, M. Heuberger, M. Vandenbossche, *Langmuir* **2016**, 32, 651.

[9] M. Vandenbossche, M.-I. Butron Garcia, U. Schütz, P. Rupper, M. Amberg, D. Hegemann, *Plasma Chem. Plasma Process.* **2016**, 36, 667.

[10] P. Rupper, M. Vandenbossche, L. Bernard, D. Hegemann, M. Heuberger, *Langmuir* **2017**, 33, 2340.

[11] [11a] S. Morgenthaler, C. Zink, N.D. Spencer, *Soft Matter* **2008**, 4, 419; [11b] P.-Y. Wang, L.R. Clements, H. Thissen, W.-B. Tsai, N. H. Voelcker, *Acta Biomater.* **2015**, 11, 58; [11c] D.J. Menzies, B. Cowie, C. Fong, J.S. Forsythe, T.R. Gengenbach, K.M. McLean, L. Puskar, M. Textor, L. Thomsen, M. Tobin, B. Muir, *Langmuir* **2010**, 26, 13987; [11d] D. Mangindaan, W.-H. Kuo, H. Kurniawan, M.-J. Wang, *J. Polym. Sci. Pol. Phys.* **2013**, 51, 1361.

[12] D. Mangindaan, W.-H. Kuo, Y.-L. Wang, M.-J. Wang, *Plasma Process. Polym.* **2010**, 7, 754.

[13] D. Mangindaan, C.-C. Kuo, S.-Y. Lin, M.-J. Wang, *Plasma Process. Polym.* **2012**, 9, 808.

[14] [14a] G. Grundmeier, M. Stratmann, *Thin Solid Films* **1999**, 352, 119; [14b] J.M. Grace, L.J. Gerenser, *J. Disper. Sci. Technol.* **2003**, 24, 305.

[15] D. Hegemann, M. Michlicek, N.E. Blanchard, U. Schütz, D. Lohmann, M. Vandenbossche, L. Zajickova, M. Drabik, *Plasma Process. Polym.* **2016**, 13, 279.

[16] D. Hegemann, E. Körner, K. Albrecht, U. Schütz, S. Guimond, *Plasma Process. Polym.* **2010**, 7, 889.
[17] D. Nečas, P. Klapetek, *Cent. Eur. J. Phys.* **2012**, 10, 181.
[18] F. Moulder, W.F. Stickle, P.E. Sobol, K.D. Bomben, *Handbook of X-ray Photoelectron Spectroscopy Physical Electronics Inc*., Eden Prairie, Minnesota USA 1995.
[19] A. Fridman, *Plasma Chemistry*, Cambridge University Press, New York USA 2008.
[20] E. Mintusov, A. Serdyuchenko, I. Choi, W.R. Lempert, I.V. Adamovich, *P. Combust. Ins.* **2009**, 32, 3181.
[21] G. Dennler, A. Houdayer, P. Raynaud, I. Séguy, Y. Ségui, M.R. Wertheimer, *Plasmas Polym.* **2003**, 8, 43.
[22] J. Benedikt, *J. Phys. D Appl. Phys.* **2012**, 43, 043001.
[23] S. Ligot, E. Bousser, D. Cossement, J. Klemberg-Sapieha, Pascal Viville, P. Dubois, R. Snyders, *Plasma Process. Polym.* **2015**, 12, 508.
[24] A.A. Leal, J.C. Veeramachaneni, F.A. Reifler, M. Amberg, D. Stapf, G.A. Barandun, D. Hegemann, R. Hufenus, *Mater. Design* **2016**, 93, 334.

Supporting information

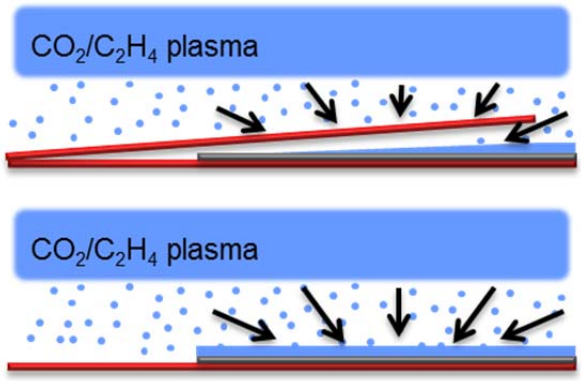

Figure S1: Scheme showing the hindered diffusion of film-forming species due to the presence of the mask compared to the diffusion of film-forming species in the usual unmasked plasma deposition process.

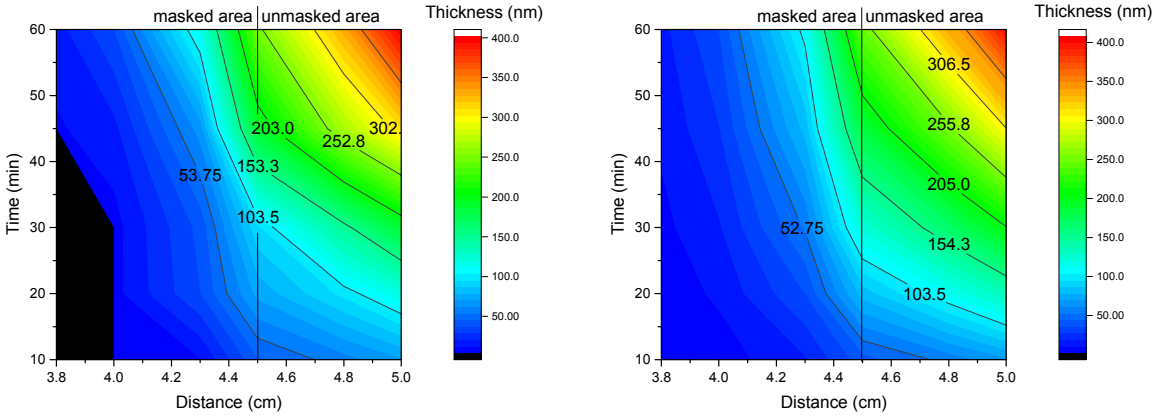

Figure S2. Contour plot images showing the measured thickness along the lateral gradient coating (left side) compared to the thickness obtained thanks to our model (right side) as a function of the position at the surface of the substrate and plasma deposition duration. The dark color indicates that the thickness was not possible to be measured in this area.

Table of Content Figure